Anhydrous crystals of DNA bases are wide gap semiconductors

Article *in* The Journal of Chemical Physics · May 2011

DOI: 10.1063/1.3584680 · Source: PubMed

6 authors, including:

Francisco Franciné Maia, Jr.
Universidade Federal Rural do Semi-Árido - UFERSA
26 PUBLICATIONS **227** CITATIONS
SEE PROFILE

Freire Valder
Universidade Federal do Ceará
313 PUBLICATIONS **2,711** CITATIONS
SEE PROFILE

Ewerton Caetano
Instituto Federal de Educação, Ciência e Tecnologia do Ceará
119 PUBLICATIONS **1,032** CITATIONS
SEE PROFILE

David Azevedo
University of Brasília
22 PUBLICATIONS **151** CITATIONS
SEE PROFILE

Anhydrous crystals of DNA bases are wide gap semiconductors

F. F. Maia Jr., V. N. Freire, E. W. S. Caetano, D. L. Azevedo, F. A. M. Sales, and E. L. Albuquerque

Citation: The Journal of Chemical Physics **134**, 175101 (2011); doi: 10.1063/1.3584680
View online: http://dx.doi.org/10.1063/1.3584680
View Table of Contents: http://scitation.aip.org/content/aip/journal/jcp/134/17?ver=pdfcov
Published by the AIP Publishing

Anhydrous crystals of DNA bases are wide gap semiconductors

F. F. Maia, Jr.,[1,2] V. N. Freire,[2] E. W. S. Caetano,[3,a)] D. L. Azevedo,[4,5] F. A. M. Sales,[2,4] and E. L. Albuquerque[4]

[1]*Universidade Federal Rural do Semi-Árido, UFERSA, Campus Angicos, 59515-000 Angicos, RN, Brazil*
[2]*Departamento de Física, Universidade Federal do Ceará, Centro de Ciências, Caixa Postal 6030, Campus do Pici, 60455-760, Fortaleza, CE, Brazil*
[3]*Instituto Federal de Educação, Ciência e Tecnologia do Ceará, 60040-531 Fortaleza, CE, Brazil*
[4]*Departamento de Biofísica e Farmacologia, UFRN, 59072-970 Natal, RN, Brazil*
[5]*Departamento de Física, Universidade Federal do Maranhão, Campus do Bacanga, 65080-040, São Luís, Maranhão, Brazil*

(Received 22 November 2010; accepted 12 April 2011; published online 5 May 2011)

We present the structural, electronic, and optical properties of anhydrous crystals of DNA nucleobases (guanine, adenine, cytosine, and thymine) found after DFT (Density Functional Theory) calculations within the local density approximation, as well as experimental measurements of optical absorption for powders of these crystals. Guanine and cytosine (adenine and thymine) anhydrous crystals are predicted from the DFT simulations to be direct (indirect) band gap semiconductors, with values 2.68 eV and 3.30 eV (2.83 eV and 3.22 eV), respectively, while the experimentally estimated band gaps we have measured are 3.83 eV and 3.84 eV (3.89 eV and 4.07 eV), in the same order. The electronic effective masses we have obtained at band extremes show that, at low temperatures, these crystals behave like wide gap semiconductors for electrons moving along the nucleobases stacking direction, while the hole transport are somewhat limited. Lastly, the calculated electronic dielectric functions of DNA nucleobases crystals in the parallel and perpendicular directions to the stacking planes exhibit a high degree of anisotropy (except cytosine), in agreement with published experimental results. © *2011 American Institute of Physics*. [doi:10.1063/1.3584680]

I. INTRODUCTION

Guanine (G), adenine (A), cytosine (C), and thymine (T) nucleotide bases are the essential building blocks of DNA (deoxyribonucleic acid), which contains the genetic information used to build living cells. DNA strands are also promising candidates to fabricate molecular nanodevices, since they are stable polymers easy to replicate. Almost ten years after the elucidation of the helical DNA structure in the landmark work of Watson and Crick,[1] where the coupling of nucleobases through hydrogen bonds and van der Walls forces has a fundamental role, Eley and Spivey[2] argued that $\pi - \pi$ interactions between stacked base pairs in double-stranded DNA could provide a pathway for rapid, one-dimensional charge separation. This early suggestion of the possibility of using DNA as a nanoscale conductor drove considerable research efforts, unfortunately without arriving to a definitive conclusion. As resumed by Gervasio *et al.*,[3] recent experiments have provided contradictory results, with works suggesting that DNA is a highly conducting wire,[4] a proximity induced superconductor,[5] a semiconductor[6] or even an insulator.[7,8] Notwithstanding that, it is believed that wet DNA is a charge carrier when its length is shorter than $\simeq$20 Å,[8] while DNA helices longer than $\simeq$40 Å or in dry conditions are generally found to be insulator or wide gap semiconductors.[9]

London dispersion forces originated from electron correlation in π stacking[10–17] and hydrogen bonding[18–20] of DNA nucleobases affect the structural, electronic, optical, and transport properties of DNA strands and derived nanostructures, being determinant to obtain the features required for technological applications. The DNA nucleobases were mainly studied in vacuum[10–20] and aqueous environments,[13,21–24] with few works being published on their crystals, some focusing on the structural, electronic, and transport properties of hydrated guanine crystals[25,26] and another investigating the dielectric function of anhydrous DNA films.[27] Recently, a new generation of exchange-correlation functionals within the density functional theory (DFT) approach has been employed to provide an improved description of hydrogen bonding and van der Waals interactions in π-stacked DNA systems.[28–31]

In vacuum, earlier MP2/6-31G* *ab initio* calculations predict that the most stable stacked pair of DNA nucleobases (considering only G···G, C···C, and A···A dimers) is the G···G dimer, while the least stable is the C···C dimer,[10] a result which was obtained considering a 3.3–3.4 Å vertical separation between bases, and which agrees with the 3.3–3.5 Å value observed in crystals of DNA constituents[32] and in high-resolved oligonucleotide crystals.[33] MP2/6-31G* calculations in the complete basis set limit (CBS) corrected by the coupled-cluster method (abbreviated as CBS(T)) have shown a different stability ordering for the same set of stacked dimers,[12] with guanine being the most stable dimer and adenine the less stable one (replacing cytosine). The orientational dependence of the stacking energy is dominated by twist and rise contributions.[10,14] DFT calculations for guanine dimers in a supercell revealed that dimers connected by hydrogen bonds have dispersionless bands, which are not good for electronic transport, while stacked dimers have dispersive bands

a)Electronic mail: ewcaetano@gmail.com.

originated from $\pi - \pi$ interactions (dispersive bands create channels for charge migration).[11] Band transport may also be partially responsible for the charge mobility in nucleotide aggregates characterized by a large base-base superposition. This scheme is probably complemented by a hopping mechanism connecting spatially different regions where such base superposition occurs.[11] The *ab initio* Hartree-Fock crystal orbital method with a basis of atomic orbitals was employed by Ladik *et al.*[13] to study the electronic structure of stackings made from the four DNA nucleobases. For the valence bands, thymine and guanine (adenine and cytosine) stackings exhibited the widest (narrowest) band widths, favoring (unfavoring) the band transport of holes. For the conduction bands the picture is somewhat different, with the band widths of guanine and cytosine (adenine and thymine) stackings being the largest (smallest), aiding (difficulting) (opposing) the band transport of electrons. The DFT estimated energy gap of stacked guanine nucleobases is 7.20 eV, larger than the gap of stacked adenine nucleobases (6.87 eV), but smaller than the gaps for cytosine and thymine (both equal to 7.41 eV).[13]

Sugar-phosphate chains, water structures, and counterions contribute to enhance DNA structural stability, and promote the formation of energy levels inside the energy gap of stacked nucleobases which strongly affect DNA electronic, optical, and charge transport properties.[13,21–24] DFT calculations within the generalized gradient approximation (GGA) for the exchange-correlation energy using the BLYP functional were performed for A-type DNA with 11 base pairs and B-type DNA with 10 base pairs,[34] including base molecule, sugar, phosphoric acid, and sodium. The geometries of the A- and B-DNA crystals used in these computations were estimated through classical molecular mechanics/molecular dynamics. The electronic band structures of A-DNA showed valence (conduction) band widths of 0.081 eV for the Poly(dG)·Poly(dC) configuration and 0.244 eV for Poly(dA)·Poly(dT) (0.133 eV for Poly(dG)·Poly(dC) and 0.360 eV for Poly(dA)·Poly(dT)).[34] In the case of B-type DNA with 10 base pairs, the widths of the valence and conduction bands were estimated as 0.045 eV (0.421 eV) and 0.120 eV (0.143 eV), respectively, for Poly(dA)·Poly(dT) (Poly(dG)·Poly(dC)) strands. The calculated energy gaps were 1.249 eV (*A*-Poly(dA)·Poly(dT)), 0.824 eV (*A*-Poly(dG)·Poly(dC)), 2.743 eV (*B*-Poly(dA)·Poly(dT)), and 1.448 eV (*B*-Poly(dG)·Poly(dC)).[34]

On the other hand, other first principles studies suggest that significant charge transport in van der Waals bonded layered guanine crystals is possible along the stacking direction[25,26] due to a dispersive band energy along the $\pi - \pi$ stacking axis with predicted valence band width of 0.83 eV and a direct gap of 2.73 eV, much smaller than the 3.90 eV HOMO-LUMO energy gap of the gas-phase guanine molecule. Finally, spectroscopic ellipsometry measurements were performed using synchrotron radiation to obtain the dielectric functions of G, A, C, T films grown on hydrogen terminated Si(111) surfaces under ultra-high vacuum conditions. Guanine and adenine films exhibited strong optical anisotropy, with the ordinary ($\perp$[111]) component of the dielectric function being larger compared to the extraordinary ($\|$[111]) component, while cytosine and thymine dielectric functions were shown to be isotropic.[27]

Although the crystal structures of anhydrous thymine[35,36] and cytosine[37,38] were determined several years ago, it is remarkable that the crystal structures of anhydrous guanine and adenine were not obtained until recently due to the lack of good quality crystals.[39,40] In this work, we use the published crystallographic data for anhydrous DNA nucleobase crystals (ACrs) guanine, adenine, cytosine, and thymine, to carry out, using DFT computations, a comparative study of their structural, electronic, and optical properties, obtaining for the first time the effective masses of electrons and holes along directions parallel and perpendicular to the π-stacking planes. In fact, considering that the carrier effective masses could be very useful to model the carrier transport in DNA-based films and nanostructures, it is surprising to note the absence in the literature of any estimates on their values for crystals of DNA nucleobases. Through our computations we predict the nature of the energy band gaps of the four DNA nucleobase ACrs (if they are direct or indirect). Experimental measurements of optical absorption for each ACr were also performed and allowed us to estimate their band gaps, showing that they resemble wide gap semiconductors. Finally, the dielectric function of each crystal was obtained for different polarization planes of incident radiation and compared with available experimental data.

II. CRYSTALS AND MEASUREMENTS DESCRIPTION

Anhydrous guanine crystals are monoclinic with space group $P2_1/c$,[39] four $C_5H_5N_5O$ molecules per unit cell, and molecular stacking along (1 0 2) planes. The anhydrous adenine crystals, on the other hand, are monoclinic with eight $C_5H_5N_5$ molecules per unit cell, space group $P2_1/c$[40] and $(10-1)$ stacking planes. The anhydrous cytosine crystals are orthorhombic with four $C_4H_5N_3O$ formulae in each unit cell, space group $P2_12_12_1$[37,38] and two intercalated stacking planes (2 0 1) and (−2 0 1), which are symmetrically equivalent. Finally, anhydrous thymine crystals have four $C_5H_6N_6O_2$ molecules in each unit cell, being monoclinic with space group $P2_1/c$[35,36] and (−1 0 1) stacking planes. Guanine and adenine molecules appear twisted along the stacking direction, cytosine molecules are slided and the thymine molecules are slided and shifted, as shown both in Fig. 1 and, more clearly, in the top part of Fig. 4. The orientation of the stacked bases in these crystals has an important role on their physical properties.[14]

Nucleobase powders (guanine 98% (G11950), adenine 99% (A8626), cytosine 99% (C3506), thymine 99% (T0376)) were purchased from Sigma-Aldrich and used with no further purification, and mixed with KBr to form six pellets for each nucleobase. Experimental measurements of the UV absorption spectra for the anhydrous crystals were carried out on these pellets using a Varian Cary 5000 UV-visible NIR spectrophotometer, equipped with solid sample holders. The absorption spectrum of the samples was recorded in the 200–800 nm (50000-12500 cm^{-1}) wavelength range. The optical absorption measurements were accomplished by transmittance and the background removal was accomplished by

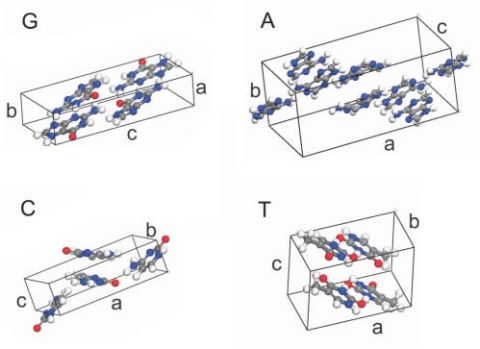

FIG. 1. Unit cells of the guanine, adenine, cytosine, and thymine anhydrous crystals.

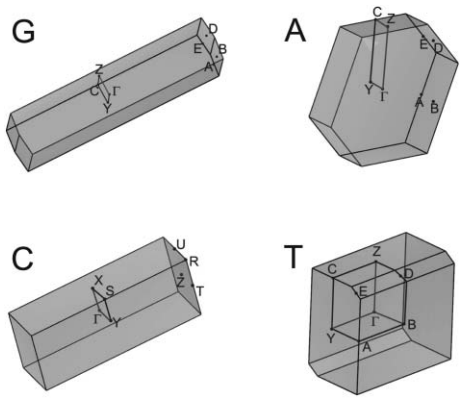

FIG. 2. First Brillouin zones of guanine, adenine, cytosine, and thymine crystals. High-symmetry points are shown.

comparison with the absorption spectrum of a KBr pellet. Baseline corrections were made when necessary.

III. COMPUTATIONAL DETAILS

The computational simulations of the present work were performed using the CASTEP code,[41,42] which is based in the DFT approach.[43,44] The local density approximation (LDA) exchange-correlation potential developed by Ceperley and Alder[45] and parametrized by Perdew and Zunger[46] was adopted as well. With respect to our choice of functional, a note of caution must be made. The LDA approximation is not the best option to provide an accurate account of hydrogen bonds, the GGA being preferable in this aspect. However, van der Waals interactions along the molecular stacking axis and hydrogen bonding between molecules in the same stacking plane are relevant to explain the structural features of anhydrous DNA bases crystals, and it is well known that pure DFT methods are unable to give a good description of dispersive forces.[28–31] Even hybrid functionals, which predict improved band gaps in comparison with LDA and GGA approaches, do not significantly improve the electronic ground state, as explained in Ref. 25. However, some DFT studies of layered crystals such as graphite as well as guanine hydrated crystals[25,47,48] have shown that the LDA gives reasonable values for atomic distances, notwithstanding the limitations of this functional. This and the relatively low cost of LDA computations have motivated us to adopt LDA instead of more sophisticated (and computationally expensive) means.

Vanderbilt ultrasoft pseudopotentials were used to describe the core electronic states of each atomic species,[49] and the Kohn-Sham orbitals were evaluated using a plane wave basis set with a converged energy cutoff of 610 eV. Each unit cell was relaxed to attain a total energy minimum allowing for lattice parameter and atomic position adjustments. Convergence thresholds selected for all geometry optimizations were: total energy variation smaller than 0.10×10^{-4} eV/atom, maximum force per atom smaller than 0.03 eV/Å, maximum displacement smaller than 0.001 Å, and maximum stress component smaller than 0.05 GPa. A two steps convergence tolerance window was employed, and the optimization method used was the BFGS minimizer.[50] The basis set quality was kept fixed throughout unit cell volume changes. The self-consistent field steps have taken into account tolerances of 0.1×10^{-5} eV/atom for total energy and 0.4979×10^{-6} eV for the electronic eigenenergies. From the valence band (VB) and conduction band (CB) curves at their critical points (maxima for VB and minima for CB) we have estimated the effective masses for electrons and holes for the anhydrous DNA bases crystals as follows: we take a band curve starting at some extremum in reciprocal space along a $\mathbf{k}$ direction of interest, and perform a parabolic fitting of this curve, which allows the determination of the corresponding effective mass through the relation $E(\mathbf{k}) = \hbar^2 k^2/2m$. For the band structure computations, paths formed from a set of high symmetry points in the first Brillouin zone were chosen, as shown in Fig. 2. However, we present here only the band structures near the valence band maxima.

IV. RESULTS AND DISCUSSION

A. Geometry optimization

From the LDA-DFT calculations, we have obtained the following formation energies for the anhydrous DNA base crystals: −60.5 kcal/mol for guanine, −42.8 kcal/mol for adenine, −47.6 kcal/mol for cytosine, and −39.4 kcal/mol for thymine, which suggests that the stability of these crystals obeys the sequence G > C > A > T. This must be put in contrast with the result of Šponer *et al.*[10,12] for guanine, adenine, cytosine, and uracil stacked dimers, which predicts a G···G dimer as the most stable stacked DNA base pair in vacuum. Moreover, stacked cytosine dimers have larger binding energy in comparison with stacked adenine dimers,[12] while our results point out that anhydrous cytosine crystals rank in second place of stability in comparison with the other crystals of DNA nucleobases (Refs. 10 and 12 have not dealt with thymine). In order to check if the distinct boundary conditions of nucleobase dimers in comparison with the crystalline phase affect the results, we have carried out LDA calculations for the same dimers studied by Šponer *et al.*,[10,12] using a 20 Å × 20 Å × 20 Å cubic supercell and the same basis set/convergence thresholds of the crystal simulations. The obtained LDA binding energies of the dimers were −10.8 kcal/mol (G···G), −7.0 kcal/mol (A···A), and −8.68 kcal/mol (C···C), which are close to the values obtained using the more accurate CBS(T) approach:

TABLE I. Calculated a, b, c lattice parameters, β angle, unit cell volume V, and distance d between successive stacked molecular planes for the guanine, adenine, cytosine, and thymine anhydrous crystals. Experimental values are indicated between parentheses and were obtained from: guanine, Ref. 39; adenine, Ref. 40; cytosine, Refs. 37 and 38; and thymine, Refs. 35 and 36.

	a (Å)	b (Å)	c (Å)	β (deg)	V (Å^3)	d (Å)
G	3.45 (3.55)	9.46 (9.69)	16.03 (16.35)	96.23 (95.75)	519.01 (560.08)	2.53 (2.59)
A	7.66 (7.89)	21.52 (22.24)	6.97 (7.45)	112.44 (113.19)	1057.86 (1201.57)	2.99 (3.19)
C	12.60 (13.04)	9.24 (9.50)	3.60 (3.81)	···	419.01 (472.42)	3.21 (3.43)
T	10.70 (12.87)	6.71 (6.83)	6.87 (6.70)	97.00 (105.00)	489.88 (568.88)	2.99 (3.19)

−12.7 kcal/mol (G···G), −8.5 kcal/mol (A···A), and −10 kcal/mol (C···C). Notwithstanding the limitations of the LDA method, its data reproduces the same ordering of dimer stabilities from the CBS(T) calculations: G···G > C···C > A···A. A direct comparison with experiment, on the other hand, is very difficult as experimental errors can be originated from a series of factors, namely: limited resolution, averaged samples, poor refinement, averaged geometries, sensitivity of hydrogen bonds, etc. However, the values reported using the CBS(T) method, as it is discussed by the authors of Ref. 12, seem to be in fair agreement with the experimental data, and the LDA values obtained here are close to the CBS(T) values. One must consider, however, that even for high level methods the calculated energies may be highly sensitive to details of the method, as the CBS(T) results disagree with previous CBS simulations,[12] so the proximity of the theoretical values to the experimental data could be only coincidental. So we hope that our numerical data will reproduce qualitative trends at least when compared with the experimental one.

The calculated lattice parameters of the ACrs are shown in Table I together with experimental data. In order to perform an analysis of these results, we define here the relative difference between theory (LDA) and experiment (Exp) for a given parameter X, $\Delta(\text{LDA} - \text{Exp}) = 100 \times (X\ \text{LDA} - X\ \text{Exp})/(X\ \text{Exp})$. It is usual for LDA computations to predict lattice parameters smaller (in comparison with Exp) by about 5% for organic crystals.[51] The figures presented in this work follow this trend. As a matter of fact, the guanine crystal has the smaller values for Δ(LDA − Exp), with LDA lattice parameters being at worst 2.9% smaller (for the a length) than the measured value. In the case of adenine, Δ(LDA − Exp) is more pronounced for the c length, which has a computed value Δ(LDA − Exp) of approximately −6.5%. For cytosine, the most pronounced difference between LDA and experiment is approximately −5.5% along c, while thymine presents the worst figures, with Δ(LDA − Exp) of −16.9% for the a parameter (a result due to the LDA overestimation of the interaction energy between thymine molecules along a direction where van der Waals forces are dominant). Also for thymine, one observe that the c parameter predicted by the LDA computations is about 2.5% larger than the experimental value, in contrast with the typical overbind trend observed for this exchange-correlation functional.

The β angle for guanine, adenine, and thymine (cytosine is orthorhombic) exhibit Δ(LDA − Exp) variations of 0.5%, −0.7%, and −7.6%, respectively (again, the worst figures are for thymine), while the unit cell volume V has Δ(LDA − Exp) of −7.3% for guanine, −12% for adenine, −11% for cytosine, and −14% for thymine. The distance between stacking planes d for each crystal has Δ(LDA − Exp) of −2.3% for guanine, −6.3% for adenine and thymine (both have practically the same value of d), and −6.4% for cytosine. The calculated d values are in general smaller than the 3.29 −3.30 Å interplanar spacing between stacked G, A, C, T dimers of <100 nm thick films grown on hydrogen terminated Si(111) surfaces under ultra-high vacuum conditions[27] and the 3.15 Å in LDA and 3.64 Å in GGA calculated intermolecular plane spacings of monohydrated guanine crystals,[25] whose experimental value is 3.30 Å.[52] Furthermore, they are practically in the range defined by the average interplanar distance of 2.56 Å and 3.38 Å in A- and B-type DNA, respectively.[34] Thus, the role of interplanar base coupling in anhydrous crystals of DNA bases on their physical properties is as relevant as in the case of stacked DNA bases, non-relaxed thick nanofilms of DNA bases, and *A*-, *B*-DNA strands.

B. Band structures

Figure 3 shows a closeup of the band structures for the ACrs at the main gap regions. Guanine and cytosine have direct band gaps, a B → B transition for the guanine crystal, and a Γ → Γ transition for cytosine. Adenine has its main band gap from a maximum at the valence band (very near to the Z point), to its conduction band minimum at the Γ point (not shown in Fig. 3), while thymine has its valence band maximum at the B point and conduction band minimum in a point in reciprocal space situated along the Γ–D direction

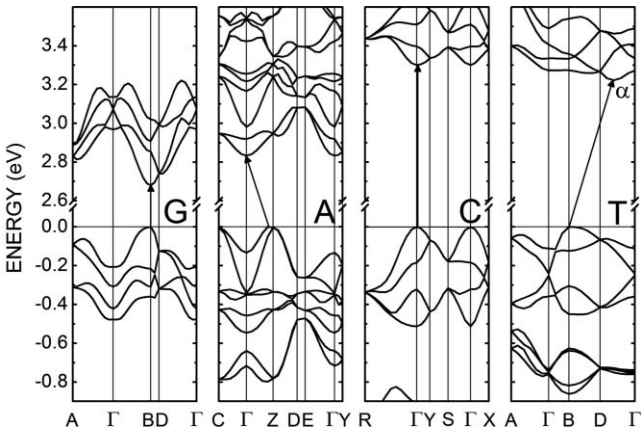

FIG. 3. Closeups of the electronic band structures of G (guanine), A (adenine), C (cytosine), and T (thymine) anhydrous crystals near their main band gaps. Direct and indirect transitions are indicated by the arrows.

TABLE II. Anhydrous crystals of DNA nucleobases: LDA and experimental energy gaps E_g with corresponding valence band → conduction band transition assigned. In the experimental section, I (D) stands for indirect (direct) gap. Effective masses of electrons and holes along directions parallel and perpendicular to the stacking planes (in units of the free electron mass m_0) are also shown.

	E_g (LDA, eV)	E_g (Exp, eV)	m_e ∥	m_e ⊥	m_h ∥	m_h ⊥
G	2.68 (B→B)	3.82−3.84[a] 2.6[b] 4.3−4.6[c]	11.5	4.0	9.2	4.0
A	2.83 (≈Z→ Γ)	3.85−3.92[a] 4.7[b] 4.5−4.6[c]	>40	5.4	>40	3.8
C	3.30 (Γ → Γ)	3.82−3.86[a] 3.6[b] 4.4−4.7[c]	>20	5.8	12	3.5
T	3.22 (B→ α)	4.04−4.09[a] 5.2[b] 4.5−4.8[c]	3.8	6.3	6.9	15

[a]This work.
[b]Reference 60.
[c]Reference 27.

(denoted here using the greek letter α), both crystals being indirect band gap materials. The main contributions for the uppermost valence bands for guanine, adenine, and cytosine originate from N 2p orbitals, while for thymine the electronic states at the top of the valence band are formed mainly from C 2p states. All nucleobases have the bottom of the conduction band formed mainly from C 2p states, with small contributions from H 1s orbitals.

Table II presents the LDA band gaps for the nucleobase crystals, together with the results of three sets of experimental results. It is necessary to remember that, as Kohn-Sham eigenvalues do not give correct excitation energies,[53,54] DFT exchange-correlation functionals predict band gaps quite different from experimental values. The LDA exchange-correlation functional tends to underestimate the main gap of semiconductors and insulators by about 40%. However, some papers suggest that a rigid shift in the LDA conduction bands is just enough to provide a reasonable agreement with the more sophisticated quasi-particle GW approximation.[53,55–57] For this reason we believe that, despite the lack of accuracy of our band gap estimates, the shape of the uppermost valence band and lowermost conduction band curves (and the effective masses calculated from them) is meaningful. The ACrs ordered by increasing band gap, according with the LDA calculations, are G < A < T < C, ranging from 2.68 eV (guanine) to 3.30 eV (cytosine).

X-ray absorption and soft x-ray emission spectroscopy of the DNA nucleobases powders were performed by MacNaughton *et al.*,[60] being obtained a HOMO-LUMO energy gap of 2.6 eV for guanine, 3.6 eV for cytosine, 4.7 eV for adenine, and 5.2 eV for thymine, leading to a G < C < A < T ordering of increasing band gaps for the ACrs, which agrees with the LDA calculations only for the lowest gap guanine crystals. On the other hand, a survey of experimental measurements performed by Silaghi *et al.*[27] for DNA nucleobase films points to an energy gap of guanine in the 4.31–4.59 eV range, cytosine in the 4.40–4.70 eV range, adenine in the 4.45–4.63 eV range, and thymine in the 4.5–4.8 eV range. As these energy ranges are overlapped, it is not possible to present a list of crystals ordered by band gaps. Moreover, the electronic structure of these thin films (80–120 nm) must be affected by surface effects absent in bulk crystals.

Tight-binding transport models depend on the interaction of adjacent orbitals and the resulting band dispersion. In this approach, the description of band transport along DNA nucleobase stackings must take into account the bandwidth of the valence and conduction bands near the respective band extremes.[25] Figure 4 presents, at its bottom part, the valence (ΔV) and conduction (ΔC) bandwidths, calculated for the uppermost and lowermost overlapping valence and conduction bands, respectively. Nevertheless, an adequate description of the charge transport, even for organic crystals, can

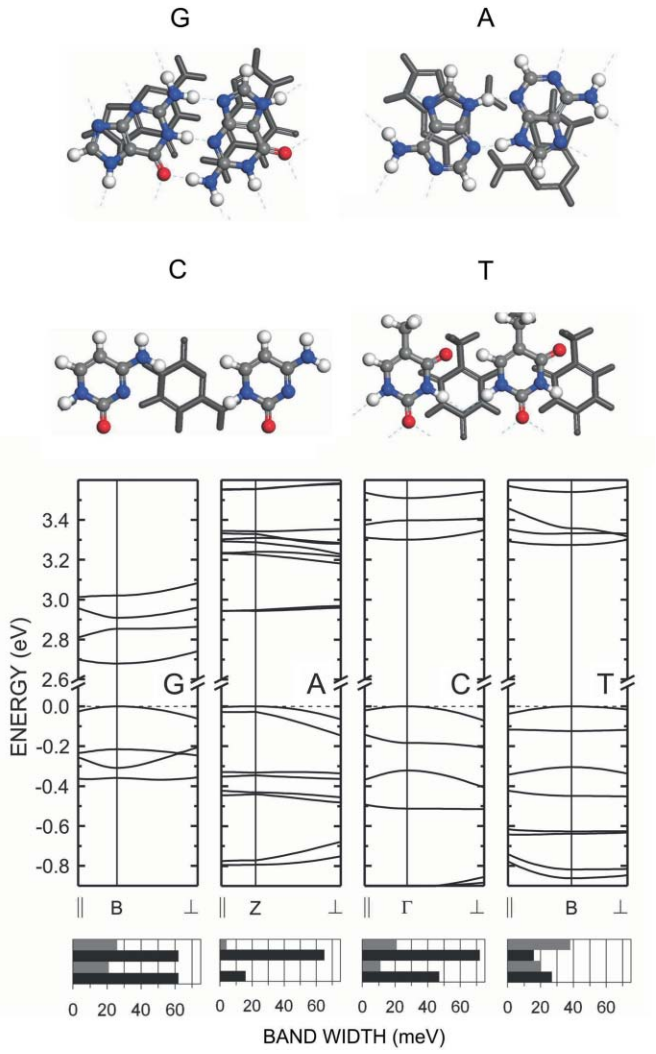

FIG. 4. Top: Viewing stacked layers in the anhydrous crystals of DNA nucleobases: G (guanine), A (adenine), C (cytosine), and T (thymine). Middle: Closeup of the G, A, C, and T band structures at the corresponding valence band maxima along directions parallel and perpendicular to the stacking planes. Bottom: G, A, C, and T valence (ΔV) and conduction (ΔC) bandwidths. In gray (black), bandwidths along the parallel (perpendicular) direction. The top two bars indicate ΔV and the two bottom bars indicate ΔC.

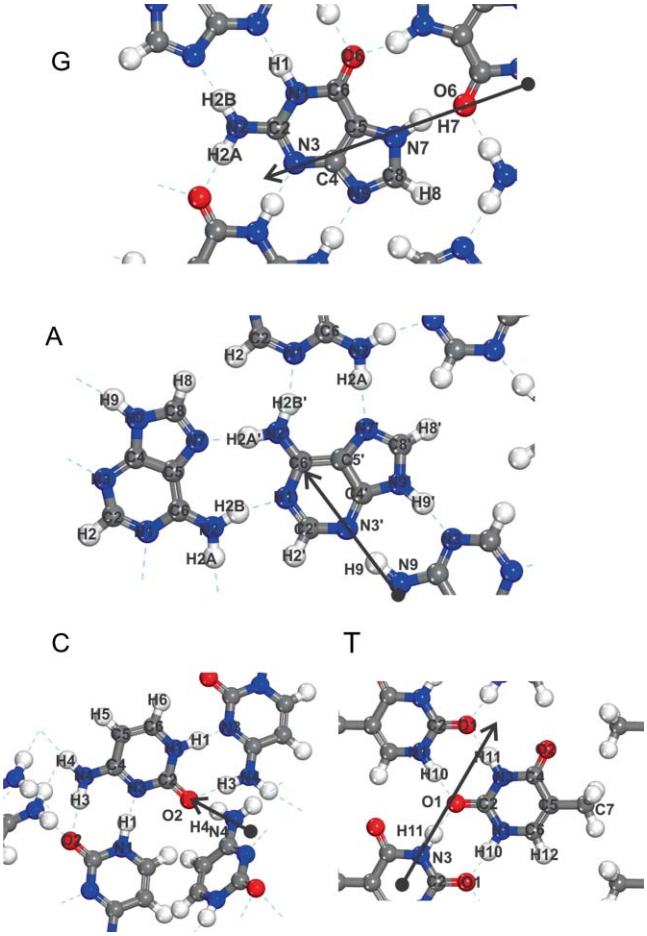

FIG. 5. "Parallel" directions along with the carrier effective masses were calculated in this work. They were chosen to be aligned with selected hydrogen bonds.

be also given through the effective mass approximation.[66] Indeed, there is a relationship between effective mass (m) and bandwidth (ΔE): the larger the first, smaller the latter (the effective mass is inversely proportional to band curvature and, therefore, to band dispersion).

The top part of Fig. 4 shows some views of the molecular layers in each ACr. Its middle part display another set of closeups of the ACrs electronic band structures near their valence band extremes for two selected directions in reciprocal space: parallel ($\parallel$) and perpendicular ($\perp$) to the plane define by a nucleobase in an unit cell. The parallel directions were selected to be along some specific hydrogen bonds in order to give some information on the transport of charge carriers across them. These directions are shown in Fig. 5: N7-H$\cdots$O6 for guanine (atomic numbering following Ref. 39), N9-H$\cdots$N3 for adenine (atomic numbering of Ref. 40), N4-H4$\cdots$O2 for cytosine (atomic numbering of Ref. 37), and N3-H$\cdots$O1 for thymine (atomic numbering of Ref. 36). These directions were used to estimate effective masses for both electrons and holes. Starting from the conduction band minimum along a direction parallel to the plan of each nucleobase, we have calculated the smallest electron effective mass for thymine (3.8 m_0, where m_0 is the free electron mass) and the largest for adenine (>40 m_0). All in all, it seems that the hopping of electrons along hydrogen bonds is very small for anhydrous crystals of guanine, adenine, and cytosine. In the perpendicular direction (along the π-stacking axis), however, all nucleobase crystals exhibit electron effective masses in the 4.0–6.3 m_0 range, signaling the possibility of semiconducting electronic transport in stacked nucleobases (for comparison, doped $SrTiO_3$ can achieve electronic effective masses as high as 7.7 m_0 (Ref. 67)). Hole transport along the parallel direction involves very large effective masses for guanine, adenine, and cytosine, while thymine has the smallest hole mass for hopping across hydrogen bonds, 6.9 m_0. For the perpendicular effective mass, this situation is reversed, with guanine, adenine, and cytosine exhibiting hole effective masses in the 3.5–4.0 m_0 range, while thymine has a 15 m_0 effective mass. In general, one can presume from the results here presented that stacked nucleobases in anhydrous crystals (and possibly for linear chains) behave like wide gap semiconductors for electrons moving along the stacking direction, while the hole transport is somewhat limited in stackings involving thymine nucleobases.

Finally, it is possible to object that the use of static structures of anhydrous crystals to obtain the electronic band structures is inadequate, as it does not take into account thermal effects which are relevant, for example, for DNA strands. Indeed, it was shown that DNA strands have electronic properties highly sensitive to DNA conformation and temperature.[61] It is more difficult, however, to include thermal effects directly into DFT calculations. Inelastic effects caused by electron-phonon coupling cannot be computed, as DFT decouples the movements of electrons and atomic nuclei following the Born-Oppenheimer approximation. Nuclear configuration effects, on the other hand, can be estimated through the sampling and averaging of an appropriate set of conformations of the studied structure, and have a more relevant role on the electronic properties of DNA base crystals. In order to make a grounded guess of the vibrational effects on the electronic structure, we have performed DFT simulations on "disturbed" crystals, with atomic positions randomly changed along arbitrary directions by 0.3 Å in average. This displacement was chosen taking as reference published data for colossal thermal expansion behavior of $Ag_3[Co(CN)_6]$ crystals, which exhibit a lattice parameter variation of about 0.3 Å in the temperature range 20–500 K,[62] and the small variation (1.7%, about 0.03 Å) of the unit cell parameters of α-glycine crystals for temperatures up to 500 K.[63,64] In comparison, thermal nuclear motions in 10–15 base pair molecules at room temperature are larger by about one order of magnitude. For all sets of crystals investigated, we noted that the shape of the valence and conduction band curves do not change significantly, at least not to the point of invalidating our conclusions on the semiconducting character of the ACrs for low temperatures, as all effective masses smaller than 7 m_0 of Table II vary by less than 1.2 m_0. One can contrast our results with those of Ortmann *et al.*,[26] who investigated the charge transport in anhydrous guanine crystals using the Kubo formalism obtaining the mobility of holes using data from DFT calculations. They have shown that the polaron concept is required to understand temperature dependence of the hole transport in guanine systems, the hole transport at room temperature having a small contribution from coherent transport and being very

anisotropic. For temperatures below about 70 K, the effective mass of hole polarons in guanine anhydrous crystals is practically constant and is about 1.5 times larger than the bare hole effective mass. Beyond this limit, the hole polaron mass increases almost linearly with temperature, reaching about 10 times the bare hole mass at 300 K. In another, more recent paper, the same authors have endorsed the use of DFT-LDA simulations to parametrize the charge transport in organic crystals for more sophisticated methods of approximation including temperature.[58] On the other hand, the band dispersion in highly ordered hydrated multilayer films of guanine was measured recently using photoelectron spectroscopy,[59] the results showing a small hole effective mass of about 1.1 m_0, suggesting the existence of band-like charge transport even at room temperature. All in all, we believe that the effective masses obtained by us are useful in the description of the low temperature charge transport (below 77 K, if we follow Ref. 58) in anhydrous DNA nucleobase crystals. Finally, besides thermal effects we could mention boundary effects, crystal defects, impurities, etc., which can also affect the electronic properties of the crystals and were not addressed here, as the present work intends to be a starting point to stimulate further research on DNA nucleobase crystals both in the experimental and theoretical frontlines.

C. Absorption spectrum and dielectric function

The averaged absorption spectra of the anhydrous nucleobase crystal powders obtained in this work are shown in Fig. 6. For each nucleobase, six samples were prepared and the average spectrum was obtained, together with the standard deviations at selected photon energies, which were used to draw the error bars. It is easy to perceive that all ACrs present two broad maxima in the energy range between about 4 and 6 eV, with the cytosine crystal exhibiting a small hump below 4 eV. As one can see, the error bars are small in general, being

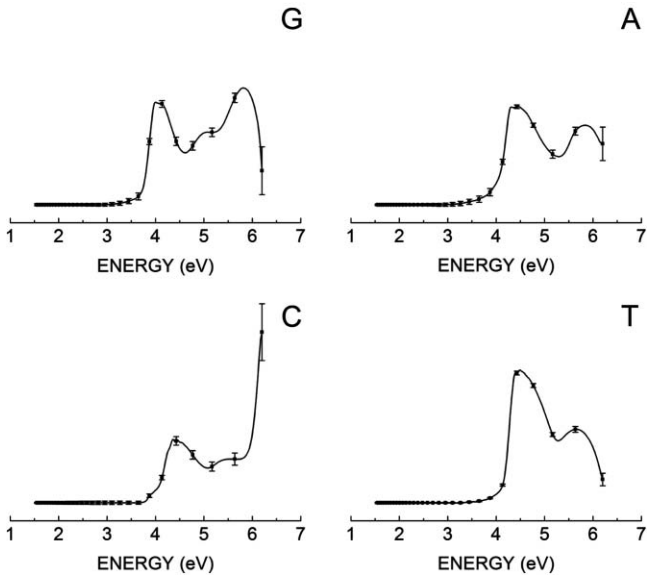

FIG. 6. Measured optical absorption spectra of the nucleobase anhydrous crystals (in arbitrary units): guanine (G), adenine (A), cytosine (C), and thymine (C). Error bars are shown for the six samples used in the experiment. Each curve is formed from 600 experimental data points.

significant only for energies larger than 6 eV, well above the onset of optical absorption. In order to estimate the energy gaps from absorption experiments, one must perform a linear fitting of the square root of the absorption coefficient near the absorption onset for direct (indirect) band gap materials.[65] Here, we used the indications given by the LDA calculations, considering that guanine and cytosine have direct band gap, while adenine and thymine have indirect band gaps. The values estimated from this interpolation (shown in Table II) comprise different, but in general small, energy ranges when one looks to the set of samples used in the measurements: 3.82–3.84 eV for guanine, 3.85–3.92 eV for adenine, 3.82–3.86 eV for cytosine, and 4.04–4.09 eV for cytosine (the difference between the maximum and minimum gap for each energy range is smaller than 0.1 eV). So, the sequence of increasing gaps is G $\approx$ C $<$ A $<$ T. Comparing this result with the order of gaps predicted by LDA computations, G $<$ A $<$ T $<$ C, we see that both data predict guanine with smallest band gap and adenine having a gap smaller than thymine, but the largest LDA band gap occurs for cytosine instead of thymine. However, taking into account the limited description of band gaps using pure DFT functionals, these differences were not surprising (one must note also that the LDA gaps we found are always smaller than the optical absorption estimates by 0.5–1 eV). We must note the gap value of Ref. 60 for guanine is slighty smaller than the LDA prediction, and much smaller than the values found from optical absorption, and the energy range proposed by Silaghi *et al.*[27] and this work. Contrasting the experimental ordering of gaps G $<$ A $<$ C $<$ T obtained by MacNaughton *et al.*[60] with ours, we see a good agreement, except that the average band gap of guanine from our absorption measurements is slightly smaller than adenine (only 10 meV), which does not allow us to affirm conclusively that guanine has the smallest band gap. The band gap of cytosine predicted in this work (average 3.84 eV) is not far from the 3.6 eV value found by MacNaughton *et al.*,[60] although the other values are very different, reaching a difference of 1.1 eV between the gaps for thymine and 1.2 eV for guanine. We believe that these differences are due to the difficulties inherent to the x-ray absorption-emission spectroscopy method employed by MacNaughton *et al.*[60] pointed out at the end of their paper: core-role effects can shift the onset of the absorption spectrum, calibration errors in the samples may occur, and the linear extrapolation method used to remove the "tail" of the spectra probably adds some uncertainty, leading to gap estimates larger or smaller by, perhaps, much more than 0.2 eV.

Figure 7 depicts the complex dielectric function for the ACrs for incident light with distinct polarizations, the real part (ε_1) being calculated from the imaginary part (ε_2) via the Kramers-Kronig relationship.[68,69] The work of Lebègue *et al.*[70] suggests that LDA dielectric functions, in comparison with more sophisticated methods, differ mainly by a scaling factor plus some energy shift. This can be checked out from our calculated curves, which after some scaling and energy shifting, compare reasonably well with the experimental data of Silaghi *et al.*[27] For guanine, there is a very pronounced anisotropy for both ε_1 and ε_2 along the polarization planes 010 (parallel to the plane of a guanine molecule), 102

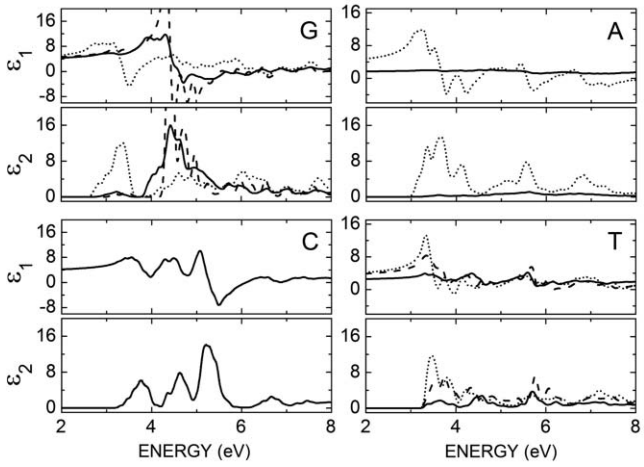

FIG. 7. Complex dielectric function, $\varepsilon = \varepsilon_1 + i\varepsilon_2$, of the anhydrous crystals of DNA bases. Solid lines: incident light with polarization plane perpendicular to the molecular plane of a single nucleobase in each ACr unit cell; dotted lines: incident light with polarization plane parallel to the nucleobase plane. Dashed lines correspond to light polarization along the $1\bar{2}\bar{8}$ plane for guanine (which contains the N7-H $\cdots$ O6 hydrogen bond) and along the $5\bar{5}2$ plane for thymine (containing the N3-H $\cdots$ O1 hydrogen bond).

(perpendicular), and $1\bar{2}\bar{8}$ (which contains the N7-H $\cdots$ O6 hydrogen bond). For adenine, the dielectric function components for light polarized along the parallel (010) and perpendicular ($10\bar{1}$) molecular planes are very anisotropic as well, with the perpendicular components exhibiting very small variation as the energy increases, which is odd, as the expected result should be a dominance of the perpendicular polarization in the optical absorption due to the transfer of electrons between neighbour π molecular orbitals. This result is probably due to the inability of the DFT-LDA functional to describe π stacking interactions. The cytosine crystal dielectric function components, on the other hand, are practically the same for light polarized along the parallel (911, containing the N4-H4 $\cdots$ O2 hydrogen bond) and perpendicular ($20\bar{1}$) molecular planes. Finally, the thymine crystals show a pronounced anisotropy for the dielectric function components when one compares the cases where the incident light is polarized parallel (010) and perpendicular (101) to the molecular plane, and parallel to the $5\bar{5}2$ plane (which contains the N3-H $\cdots$ O1 hydrogen bond). The anisotropy of the optical properties of guanine, thymine, and adenine (specially the latter) can be useful for applications in the field of nonlinear optics, for example.

V. CONCLUDING REMARKS

The stacking of identical DNA bases in anhydrous crystals is directly responsible for their semiconductor character. In DNA strands, deviations from the semiconductor character can be assigned to the influence of sugar-phosphate chains, water structures as well as counterions.[9] A direct band gap of 2.73 eV was obtained for monohydrated guanine crystals through LDA first-principles calculations,[25] a little higher than the direct band gap of 2.68 eV we have obtained for anhydrous guanine crystals. In this case, we can not suggest yet that water molecules contribute to increase the energy gap because details on the calculations procedures and figures, as wells well as the different softwares employed by us and Ortmann *et al.*[25] can change easily the estimated value of the band gap of monohydrated guanine crystals. However, our study points that a sound picture of the role of water can be achieved by comparing the structural, electronic, and optical properties of monohydrated and anhydrous crystals of DNA nucleobases through the same computational methodology, a work already being undertaken by the authors.

In summary, we have performed DFT calculations to obtain optimized geometries for the anhydrous crystals of the four DNA nucleobases, guanine (G), adenine (A), cytosine (C), and thymine (T) using the LDA for the exchange-correlation functional, and have estimated the band gaps of these crystals from optical absorption measurements. The LDA optimized crystals have lattice parameters smaller than experimental values, with the smallest (b parameter, -1.7%) and largest (a parameter, $\approx -17\%$, resulting from the LDA overestimation of the interaction along a direction where van der Waals forces are preponderant) differences observed for the thymine crystal. The distance between molecular planes d is 2.3% smaller than experiment for guanine and 6.4% smaller for cytosine. The difference between experimental data and the optimized unit cell volumes increases in the order G < C < A < T. This same ordering is followed by the formation energies of the crystals, suggesting that guanine is the most stable structure, while thymine is the less stable. Analysis of the electronic band structures of the ACrs revealed that guanine and cytosine are direct band gap materials, while adenine and thymine have indirect band gaps. LDA figures for the energy gaps are smaller than experimental values, as expected, and the gaps estimated from the optical absorption measurements presented in this work are in general smaller than experimental data available in the literature (except for guanine). The LDA ordering of increasing band gaps is G < A < C < T, while the ordering obtained from the optical absorption measurements is G $\approx$ C < A < T. Band dispersions, which are crucial to model the electronic transport using the tight-binding approach, are related with the effective masses, which were are also calculated in this work. For electrons and holes moving along selected hydrogen bonds (parallel to the molecular plane of a given nucleobase), effective masses are in general large, exception made to thymine. When the same electrons move along the π-stacking axis, however, the effective masses stay in the 4.0–6.3 m_0 range, which suggests that stackings of nucleobases at low temperature behave like wide gap semiconductors for electrons. The transport of holes is also favored for nucleobase stackings without thymine. Finally, the complex dielectric function was calculated for each ACr, and a very pronounced anisotropy was observed for polarized incident light in the cases of guanine, thymine, and for adenine (specially), but not for cytosine.

ACKNOWLEDGMENTS

E.L.A. and V.N.F. are senior researchers from the Brazilian National Research Council (CNPq), and would like to acknowledge the financial support received during the development of this work from the Brazilian

Research Agencies CAPES-PROCAD and Rede Nanobiotec, CNPq-INCT-Nano(Bio)Simes project 573925/2008-9, and FAPERN-CNPq (Pronex). E.W.S.C. received financial support from CNPq projects 304338/2007-9 and 482051/2007-8.

[1] J. D. Watson and F. H. C. Crick, Nature (London) **171**, 964 (1953).
[2] D. D. Eley and D. I. Spivey, Trans. Faraday Soc. **58**, 411 (1962).
[3] F. L. Gervasio, A. Laio, M. Parrinello, and M. Boero, Phys. Rev. Lett. **94**, 158103 (2005).
[4] R. Holmlim, P. Dandliker, and J. Barton, Angew. Chem. Int. Ed. Engl. **36**, 2714 (1997).
[5] A. Yu. Kasumov, M. Kociak, S. Guéron, B. Reulet, V. T. Volkov, D. V. Klinov, and H. Bouchiat, Science **291**, 280 (2001).
[6] D. Porath, A. Bezryadin, S. deVries, and C. Dekker, Nature (London) **403**, 635 (2000).
[7] P. J. de Pablo, F. Moreno-Herrero, J. Colchero, J. Gómez Herrero, P. Herrero, A. M. Baró, P. Ordejón, J. M. Soler, and E. Artacho, Phys. Rev. Lett. **85**, 4992 (2000).
[8] C. Gómez-Navarro, F. Moreno-Herrero, P. J. de Pablo, J. Colchero, J. Gómez Herrero, and A. M. Barró, Proc. Natl. Acad. Sci. U.S.A. **99**, 8484 (2002).
[9] R. G. Endres, D. L. Cox, and R. R. P. Singh, Rev. Mod. Phys. **76**, 195 (2004).
[10] J. Šponer, J. Leszczyński, and P. Hobza, J. Phys. Chem. **100**, 5590 (1996).
[11] R. Di Felice, A. Calzolari, E. Molinari, and A. Garbesi, Phys. Rev. B **65**, 045104 (2001).
[12] J. Šponer, K. E. Riley, and P. Hobza, Phys. Chem. Chem. Phys. **10**, 2595 (2008).
[13] J. Ladik, A. Bendem, and F. Bogár, J. Chem. Phys. **128**, 105101 (2008).
[14] Z. Czyżnikowska, J. Mol. Struct. **895**, 161 (2009).
[15] A. Calzolari, R. Di Felice, and E. Molinari, Solid State Commun. **131**, 557 (2004).
[16] A. Robertazzi and J. A. Platts, J. Phys. Chem. A **110**, 3992 (2006).
[17] V. R. Cooper, T. Thonhauser, A. Puzder, E. Schröder, B. I. Lundqvist, and D. C. Langreth, J. Am. Chem. Soc. **130**, 1304 (2008).
[18] C. F. Guerra, F. M. Bickelhaupt, J. G. Snidjers, and E. J. Baerends, J. Am. Chem. Soc. **122**, 4117 (2000).
[19] A. Sadowska-Aleksiejew, J. Rak, and A. A. Voityuk, Chem. Phys. Lett. **429**, 546 (2006).
[20] Y. Mo, J. Mol. Model. **12**, 665 (2006).
[21] F. L. Gervasio, P. Carloni, and M. Parinello, Phys. Rev. Lett. **89**, 108102 (2002).
[22] A. Hübsch, R. G. Endres, D. L. Cox, and R. R. P. Singh, Phys. Rev. Lett. **94**, 178102 (2005).
[23] R. N. Barnett, C. L. Cleveland, U. Landman, E. Boone, S. Kanvah, and G. B. Schuster, J. Am. Chem. Soc. **107**, 3225 (2003).
[24] M. Kabeláč and P. Hobza, Phys. Chem. Chem. Phys. **9**, 903 (2007).
[25] F. Ortmann, K. Hannewald, and F. Bechstedt, J. Phys. Chem. B **112**, 1540 (2008).
[26] F. Ortmann, K. Hannewald, and F. Bechstedt, J. Phys. Chem. B **113**, 7367 (2009).
[27] S. D. Silaghi, M. Friedrich, C. Cobet, N. Esser, W. Braun, and D. R. T. Zahn, Phys. Status Solidi B **242**, 3047 (2005).
[28] Y. Zhao and D. G. Truhlar, Phys. Chem. Chem. Phys. **7**, 2701 (2005).
[29] T. van der Wijst, C. F. Guerra, M. Swart, and F. M. Bickelhaupt, Chem. Phys. Lett. **426**, 415 (2006).
[30] V. R. Cooper, T. Tronhauser, and D. C. Langreth, J. Chem. Phys. **128**, 204102 (2008).
[31] P. L. Silvestrelli, J. Phys. Chem. A **113**, 5224 (2009).
[32] C. E. Bugg, J. M. Thomas, M. Sundaralingam, and S. T. Rao, Biopolymers **10**, 175 (1971).
[33] J. Šponer and J. Kypr, J. Biomol. Struct. Dyn. **11**, 277 (1993).
[34] M. Taniguchi and T. Kawai, Phys. Rev. E **70**, 011913 (2004).
[35] K. Ozeki, N. Sakabe, and J. Tanaka, Acta Crystallogr., Sect. B: Struct. Crystallogr. Cryst. Chem. **25**, 1038 (1969).
[36] G. Portalone, L. Bencivenni, M. Colapietro, A. Pieretti, and F. Ramondo, Acta Chem. Scand. **53**, 57 (1999).
[37] R. J. McClure and B. M. Craven, Acta Crystallogr., Sect. B: Struct. Crystallogr. Cryst. Chem. **29**, 1234 (1973).
[38] D. L. Barker and R. E. Marsh, Acta Crystallogr. **17**, 1581 (1964).
[39] K. Guille and W. Clegg, Acta Crystallogr., Sect. C: Cryst. Struct. Commun. **62**, o515 (2006).
[40] S. Mahapatra, S. K. Nayak, S. J. Prathapa, and T. N. G. Row, Cryst. Growth Des. **8**, 1223 (2008).
[41] M. C. Payne, M. P. Peter, D. C. Allan, T. A. Arias, and J. D. Joannopoulos, Rev. Mod. Phys. **64**, 1045 (1992).
[42] M. D. Segall, P. J. D. Lindan, M. J. Probert, C. J. Pickard, P. J. Hasnip, S. J. Clark, and M. C. Payne, J. Phys. Condens. Matter **14**, 2717 (2002).
[43] P. Hohenberg and W. Kohn, Phys. Rev. B **136**, 864 (1964).
[44] W. Kohn and L. J. Sham, Phys. Rev. A **140**, 1133 (1965).
[45] D. M. Ceperley and B. J. Alder, Phys. Rev. Lett. **45**, 566 (1980).
[46] J. P. Perdew and A. Zunger, Phys. Rev. B **23**, 5048 (1981).
[47] F. Ortmann, W. G. Schmidt, and F. Bechstedt, Phys. Rev. Lett. **95**, 186101 (2005).
[48] F. Ortmann, F. Bechstedt, and W. G. Schmidt, Phys. Rev. B **73**, 205101 (2006).
[49] D. Vanderbilt, Phys. Rev. B **41**, 7892 (1990).
[50] B. G. Pfrommer, M. Cote, S. G. Louie, and M. L. Cohen, J. Comput. Phys. **131**, 233 (1997).
[51] K. Hannewald, V. M. Stojanović, J. M. T. Schellekens, P. A. Bobbert, G. Kresse, and J. Hafner, Phys. Rev. B **69**, 075211 (2004).
[52] U. Thewalt, C. E. Bugg, and R. E. Marsh, Acta Crystallogr., Sect. B: Struct. Crystallogr. Cryst. Chem. **27**, 2358 (1971).
[53] R. W. Godby, M. Schlüter, and L. J. Sham, Phys. Rev. B **37**, 10159 (1988).
[54] J. P. Perdew and M. Levy, Phys. Rev. Lett. **51**, 1884 (1983).
[55] Z. H. Levine and D. C. Allan, Phys. Rev. B **43**, 4187 (1991).
[56] U. Schönberger and F. Aryasetiawan, Phys. Rev. B **52**, 8788 (1995).
[57] S. Q. Wang and H. Q. Ye, J. Phys.: Condens. Matter **15**, L197 (2003).
[58] F. Ortmann, F. Bechstedt, and K. Hannewald, Phys. Status Solidi B **248**, 511 (2011).
[59] R. Friedlein, Y. Wang, A. Fleurence, F. Bussolotti, Y. Ogata, and Y. Yamada-Takamura, J. Am. Chem. Soc. **132**, 12808 (2010).
[60] J. MacNaughton, A. Moewes, and E. Z. Kurmaev, J. Phys. Chem. B **109**, 7749 (2005).
[61] D. N. Beratan, S. S. Skourtis, I. A. Balabin, A. Balaeff, S. Keinan, R. Venkatramani, and D. Q. Xiao, Acc. Chem. Res. **42**, 1669 (2009).
[62] A. L. Goodwin, M. Calleja, M. J. Conterio, M. T. Dove, J. S. O. Evans, D. A. Keen, L. Peters, and M. G. Tucker, Science **319**, 794 (2008).
[63] C. P. Schwartz, R. J. Saykally, and D. Prendergast, J. Chem. Phys. **133**, 044507 (2010).
[64] P. Langan, S. A. Mason, D. Myles, and B. P. Schoenborn, Acta Crystallogr., Sect. B: Struct. Sci. **58**, 728 (2002).
[65] M. Fox, *Optical Properties of Solids* (Oxford University Press, New York, 2001).
[66] K. Hummer, C. Ambrosh-Draxl, Phys. Rev. B **72**, 205205 (2005).
[67] W. Wunderlich, H. Ohta, and K. Koumoto, Physica B **404**, 2202 (2009).
[68] H. A. Kramers, *Atti del Congresso Internazionale dei Fisici* (Zanichelli, Bologna, 1927), Vol. 2, p. 545.
[69] R. de L. Kronig, J. Opt. Soc. Am. **12**, 547 (1926).
[70] S. Lebègue, B. Arnaud, and M. Alouani, Phys. Rev. B **72**, 085103 (2005).